Article

Impact of Zeolite from Coal Fly Ash on Soil Hydrophysical Properties and Plant Growth

Claudia Belviso [1,*], Antonio Satriani [1], Stella Lovelli [2], Alessandro Comegna [2], Antonio Coppola [2], Giovanna Dragonetti [3], Francesco Cavalcante [1] and Anna Rita Rivelli [2]

1 Istituto di Metodologie per l'Analisi Ambientale—IMAA-CNR, Tito Scalo (PZ), 85050 Potenza, Italy; antonio.satriani@imaa.cnr.it (A.S.); francesco.cavalcante@imaa.cnr.it (F.C.)
2 School of Agricultural, Forest, Food and Environmental Sciences, University of Basilicata, 85100 Potenza, Italy; stella.lovelli@unibas.it (S.L.); alessandro.comegna@unibas.it (A.C.); antonio.coppola@unibas.it (A.C.); annarita.rivelli@unibas.it (A.R.R.)
3 Mediterranean Agronomic Institute, Land and Water Division, IAMB, 70010 Bari, Italy; dragonetti@iamb.it
* Correspondence: claudia.belviso@imaa.cnr.it

Abstract: Zeolites can be extensively employed in agricultural activities because they improve soil properties such as infiltration rates, saturated hydraulic conductivity, water holding capacity, and cation exchange capacity. Natural and synthetic zeolites can efficiently hold water. Zeolites are also believed to have the ability to lose and gain water reversibly, without changing their crystal structure. In the present study, several laboratory tests were carried out using: (i) zeolite synthesized from coal fly ash (a waste product from burning coal in thermoelectric power plants), (ii) a silty loam soil, typically found in Southern Italy, and (iii) sunflower as a reference plant. The selected soil was amended with different percentages of zeolite (1, 2, 5, and 10%) and the effects of the synthetic mineral addition on the hydrophysical properties of the soil and plant growth were evaluated. The results indicated that soil–zeolite mixtures retained water more efficiently by pore radius modification. However, this causes a variation in the range of plant-available water towards higher soil humidity values, as the amount of added zeolite increases. These data confirm that zeolite addition modifies the selected hydrophysical properties of the soil with the effect of decreasing the soil drainage capacity, making the soil less habitable for plant growth.

Keywords: zeolites; waste; fly ash; water scarcity; irrigation; water holding capacity; soil hydrophysical properties

1. Introduction

More than two-thirds of renewable water resources are used in agricultural activities [1,2]. Water resources are becoming inadequate, particularly in arid and semi-arid regions, where such scarcity represents one of the most important issues that can affect the development of agriculture [3–7]. In recent years, several agronomic strategies (e.g., drip-irrigation, partial root zone drying, deficit irrigation) and innovative materials (e.g., biochar and superabsorbent polymers) have been widely shown to improve soil capacity to retain water with ensuing positive effects on plant growth and production [8–12].

Due to their high cation exchange capacity (CEC) and high water adsorption, zeolites have also been used in agriculture [13,14]. Zeolites are aluminosilicate minerals occurring in nature or synthesized using different raw materials including pure sources, other minerals, and wastes [15–23]. The efficiency of zeolites in improving plant growth due to the positive effect on the long-term availability of both water and nutrients has been extensively analyzed [24–29]. In their review, Nakhli et al. [30] summarized and discussed the recent findings concerning the impact of zeolites on water retention in soil. The authors analyzed the effects of zeolites on infiltration rate, hydraulic conductivity, soil water content and nutrient retention, concluding that both natural and synthetic zeolites affect the above soil

properties. Zeolites may also change the physical properties of soil such as total porosity, bulk density, and structure [31]. Moreover, due to their porous structure characterized by open pore network channels, zeolites can enhance the water holding capacity in soils [32,33] and increase the amount of available water in sandy soils [34].

The action of zeolites in both leaching reduction and the adsorption amount of NH_4^+ in soil has also been explored [35–38]. Shahsavari [22] analyzed the positive effects on plant growth resulting from the application of natural zeolites combined with zinc in soil under drought stress conditions. The efficiency of zeolites in agriculture was also described by Polat et al. [39] who displayed the positive role of clinoptilolite in reducing N and K fertilizer rates due to its ability to retain these nutrients and make them available to the plant when needed. Ozbahce et al. [40] tested the efficiency of natural zeolite clinoptilolite combined with different irrigation levels on potato growth, showing the positive effects of different zeolite doses on tuber yield and quality under water deficit conditions. Bahador and Tadayon [41] demonstrated that zeolite application reduces the negative impact of water deficit on industrial plants such as hemp. The authors showed that under different water deficit conditions, zeolite has effects on antioxidant enzymes in leaves and carotenoid content. Moreover, when used at a rate of 10 t ha^{-1}, zeolite addition compensates for the negative impact of water deficiency on defense systems in hemp.

Zeolites synthesized from coal fly ash (FA), a waste product of burning coal in thermo-electric power plants, have also been successfully applied in agriculture [42]. Ayan et al. [43] studied the positive effects of zeolites from FA in enhancing plant nutrient retention as well as in regulating the water supply when amended in soil. Additionally, Flores et al. [44] demonstrated that merlinoite, formed from coal fly ash, can be positively used as potassium fertilizer in agriculture

However, despite the fairly large number of research studies describing the positive effects of natural zeolites in agricultural practices, few studies have investigated the ability of zeolite formed from waste materials to affect the water holding capacity linked to plant growth, and most of these studies concern sandy soils. In our study, several experiments were carried out using different amounts of zeolite synthesized from coal fly ash and a silty loam soil, typically found in Southern Italy. Sunflower was chosen as a reference plant. The objective was to evaluate the effects of different soil–zeolite mixtures (1, 2, 5, and 10% of zeolite was added to the soil) on the hydrophysical properties of the soil and plant growth starting from the hypothesis that the addition of an increasing amount of zeolite impacts soil porosity, saturated hydraulic conductivity, and the water holding capacity of soils.

2. Materials and Methods

2.1. Soil and Zeolite Characterization

The soil used in the present study was collected at the experimental agricultural farm "Pantano di Pignola" (40°33′31″ N and 15°45′31″ E; 800 m above sea level) of ALSIA (Agency for the Agricultural Development and Innovation of Lucania) in Basilicata Region, Southern Italy, characterized by a warm summer Mediterranean climate (Koppen climate classification Csb) [45]. The main physicochemical properties of the soil are shown in Table 1. All the properties were determined using standard laboratory protocols based on the methods of chemical and physical analysis described in the Italian Official Gazette [46]. The soil was classified as a silty loam [47], hereinafter referred to as SiLo. It was characterized by the large amount of organic matter (34.9 g kg^{-1}), exchangeable Ca^{2+} (4852 mg kg^{-1}), and available P (53.02 mg kg^{-1}). The quantity of available Fe was 9.98 mg kg^{-1} (Table 1).

Table 1. Main physicochemical properties of the investigated soil.

Property	Soil	Unit	Method
Sand	9.53	%	
Silt	66.18	%	hydrometer method
Clay	24.29	%	
Texture (USDA classification)	Silty loam	-	
Soil bulk density (ρ_b)	1.369	g/cm^3	core method
Field capacity (FC)	40.5	%	retention curve (at $h = -0.03$ MPa)
Wilting point (WP)	25.5	%	retention curve (at $h = -1.5$ MPa)
pH (in H$_2$O 1:2.5)	7.63		pH meter
Cation exchange capacity	27.85	cmol/kg	BaCl$_2$ pH 8.1
Organic matter	34.90	g kg^{-1}	Walkley–Black
Exchangeable K$^+$	317	mg kg^{-1}	BaCl$_2$ pH 8.1
Exchangeable Mg^{2+}	277	mg kg^{-1}	BaCl$_2$ pH 8.1
Exchangeable Ca^{2+}	4852	mg kg^{-1}	BaCl$_2$ pH 8.1
Fe	9.98	mg kg^{-1}	Lindsay–Norwell
Mn	5.81	mg kg^{-1}	Lindsay–Norwell
Zn	1.45	mg kg^{-1}	Lindsay–Norwell
Cu	0.99	mg kg^{-1}	Lindsay–Norwell
P	53.02	mg kg^{-1}	Olsen

The zeolite used in the laboratory experiments was synthesized from an Italian coal fly ash sample (thermoelectric power plant in Cerano-Brindisi) according to the method described in our previous papers [48] and based on the pre-fused hydrothermal process at 60 °C. The synthetic product was Ca-exchanged following the method described by Sun et al. [49]. X-ray diffraction (XRD) analysis was performed on soil, synthetic zeolite, and soil–zeolite mixtures using a Rigaku Rint 2200 powder diffractometer equipped with a CuKα radiation source. Data were collected in the 2–70° range of 2θ with a 0.02° step and a speed of 3 s/step.

2.2. Hydrophysical Characterization of the Soil–Zeolite Mixtures

Laboratory tests were performed on disturbed (i.e., repacked) soil samples to evaluate the hydrophysical behavior of the soil–zeolite mixtures. The soil was oven-dried at 105 °C and sieved at 2 mm. Known amounts of soil and zeolite were then mixed and shaken to ensure a uniform distribution. The mixtures were then kept in metallic containers of cylindrical geometry (8 cm high and 8 cm in diameter) for several steps. The experimental protocol involved four distinct soil–zeolite mixtures prepared with 1% (in the following SiLo_Z1), 2% (SiLo_Z2), 5% (SiLo_Z5), and 10% (SiLo_Z10) of zeolite. The analysis was also performed on a soil sample without zeolite (SiLo_Z0), which was used as a control. Hydraulic conductivity at saturation, K_s, was measured for each soil sample using the constant head method [50]. Soil water retention curves (SWRCs) were also determined for all the soil cores. Water retentions were obtained for the samples by first saturating the soil, from the bottom, with tap water and then drying it with a Stackman apparatus [51]. Drying was induced gradually by applying decreasing pressure heads in the range from 0–0.0245 MPa at the bottom of the soil cores.

The experimental SWRCs were fitted using the water retention model of van Genuchten [52]:

$$\theta = \theta_r + \frac{\theta_s - \theta_r}{\left[1 + \alpha|h|^n\right]^m} \tag{1}$$

where θ (cm^3/cm^3) is the volumetric water content, θ_r (cm^3/cm^3) and θ_s (cm^3/cm^3) are the residual volumetric water content and the water content at saturation, respectively, h (cm) is the pressure head, and α (1/cm), n (-) and m (-) ($m = 1 - 1/n$) are fitting parameters.

The RETC software package [53] was employed to determine van Genuchten's model parameters via a nonlinear least squares optimization approach [54]. In the RETC procedure,

θ_r is assumed to be zero. Furthermore, following the approach of Durner et al. [55] and Jensen et al. [56], pore size distribution (PSD) was also determined using the van Genuchten model by differentiating Equation (1) with respect to h:

$$f(h) = \frac{d\theta}{d(log_{10}|h|)} = (\theta_s - \theta_r)\left\{\alpha n|\alpha h|^{(n-1)} - m\left[1 + (\alpha|h|)^n\right]^{-(m+1)}\right\}|h|ln10 \qquad (2)$$

where $f(h)$, known as the pore capillary pressure distribution function, is obtained on the basis of the direct correspondence (equation of Young–Laplace) of h and the pore radius r [57]. The PSD function is the first derivative of the SWRC and expresses the relative abundance of each pore size in a representative volume of soil, that is the statistical frequency distribution of pore sizes in the material under study. The function is usually defined in the $\theta_r < \theta < \theta_s$ range [58].

2.3. Plant Growth Experiment

The experiment was carried out at the University of Basilicata (Southern Italy) in Potenza on sunflower (*Helianthus annuus* L. cv Talento) grown in a temperature-controlled glasshouse. The day/night temperatures were 26/23 °C and relative humidity was 40%. Pregerminated sunflower seeds were sown singly in plastic pots (each 10 L) containing 7 kg of soil (air-dried and passed through a 2-mm sieve whose characteristics are shown in Table 1) treated with different percentages of zeolite (0, 1, 2, 5, and 10%). The plant growth experiment was a randomized complete block design with six replications and five treatments for a total of 30 pots. Plants were fertilized with potassium nitrate (1.5 g of N plant^{-1}) and diammonium phosphate (1.6 g of P_2O_5 plant^{-1}). During the growing cycle, plants were irrigated weekly by reestablishing field capacity (Table 1), whose water requirement was obtained by gravimetric measures. From leaf emergence to the flower bud stage, plants were monitored by counting the leaf number and measuring plant height (H). In addition, measurements of the leaf greenness index (SPAD) were made by using a handheld Soil Plant Analysis Development—SPAD-502 (Konica Minolta Corporation, Ltd., Osaka, Japan). Average SPAD meter values were calculated from three readings taken from the tip to the base of the youngest and fully expanded leaf per plant. Moreover, gas exchange parameters (photosynthesis, transpiration, stomatal conductance, and intercellular CO_2 concentration) were measured using a LI-6400 portable photosynthesis system equipped with a 2 cm^2 chamber and 6400-40 LED light source (LI-COR Inc.) operating at 380 ppm ambient CO_2 concentration. Measurements were carried out between 12:00 and 14:00 h (solar time) under saturating light conditions (photosynthetic active radiation, PAR approximately 1500 μmol photons m^{-2} s^{-1}).

At the end of the experiment, when the sunflower was at the flower bud stage, the plant was harvested and weighed to determine fresh weight (FW). The leaves were counted and passed through a surface electronic detector (Model 3100, LI-Cor, Inc., Lincoln, NE, USA) to measure leaf area. Finally, dry weight (DW), by drying the samples in a ventilated oven at 75 °C until constant weight was reached, and humidity (%) were determined.

2.4. Statistical Analysis

Hydrophysical soil and plant growth parameters were analyzed by one-way ANOVA statistical test. When significant treatment effects were found, the Duncan Multiple Range Test (DMRT) was used to compare the obtained mean values among the treatments. These mean values were considered to be significantly different at $p \leq 0.05$ and $p \leq 0.01$.

3. Results and Discussion

3.1. Soil and Synthesized Zeolites

The mineralogical composition of the SiLo soil used during the experiments is displayed in Figure 1. The XRD pattern indicates that it was characterized by the presence of quite large amounts of clay minerals represented by kaolinite, chlorite, illite/mica, and mixed-layer illite/smecite. Other minerals such as quartz, calcite, and a smaller amount of

dolomite and feldspars were also present. Peaks referable to goethite/hematite, were well identifiable. Figure 2 shows the XRD profile of synthetic zeolites characterized by the main presence of sodalite whose addition in treatments with a higher percentage (SiLo_Z5 and SiLo_Z10) is clearly shown in Figure 3. Zeolite percentages of 1% and 2% (SiLo_Z1 and SiLo_Z2) were, instead, too low to be determined by X-ray diffraction (Figure 3). The results indicate that the addition of sodalite, formed from a waste material such as coal fly ash into silty loam soil, conditions its hydrophysical properties and sunflower growth, although, the quantity of clay minerals was not negligible and the amount of added synthetic zeolite was so low it was not detected by XRD analysis (Figure 3).
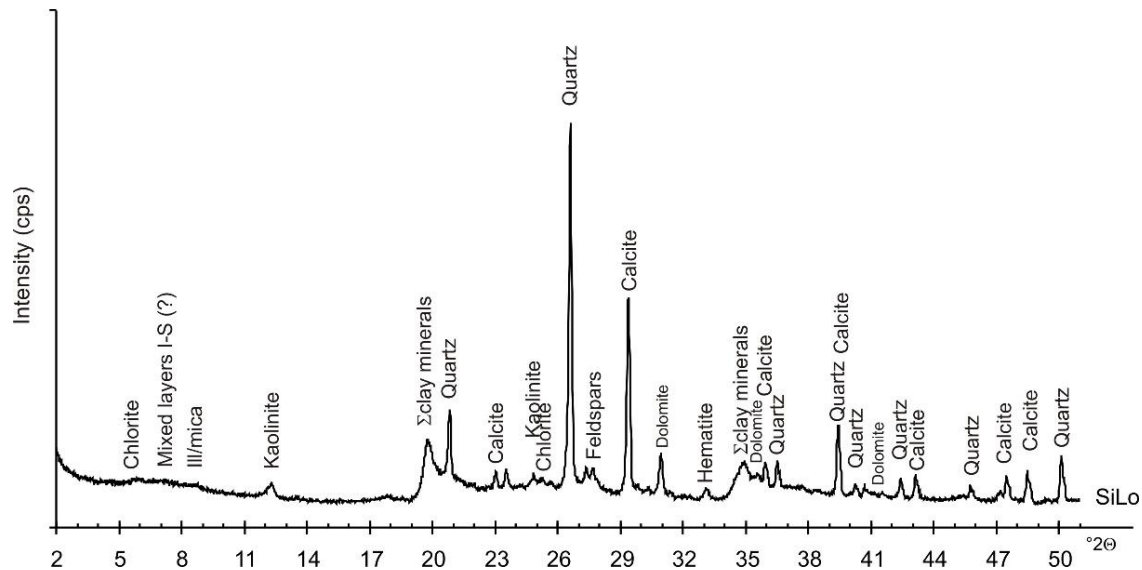

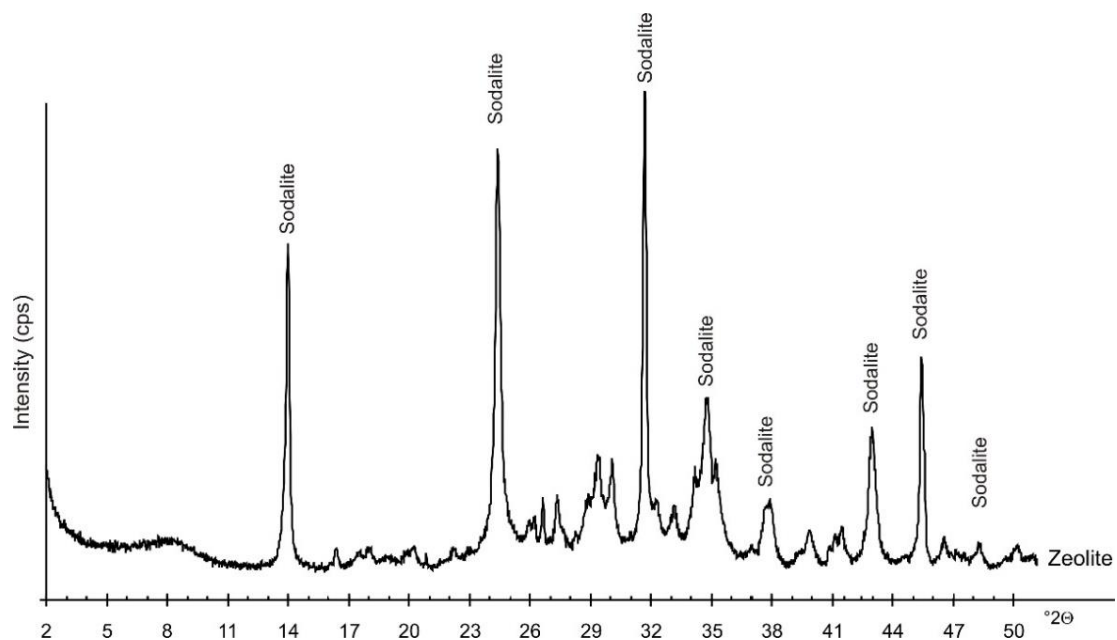**Figure 1.** X-ray pattern of the soil (SiLo) used in the experiments.

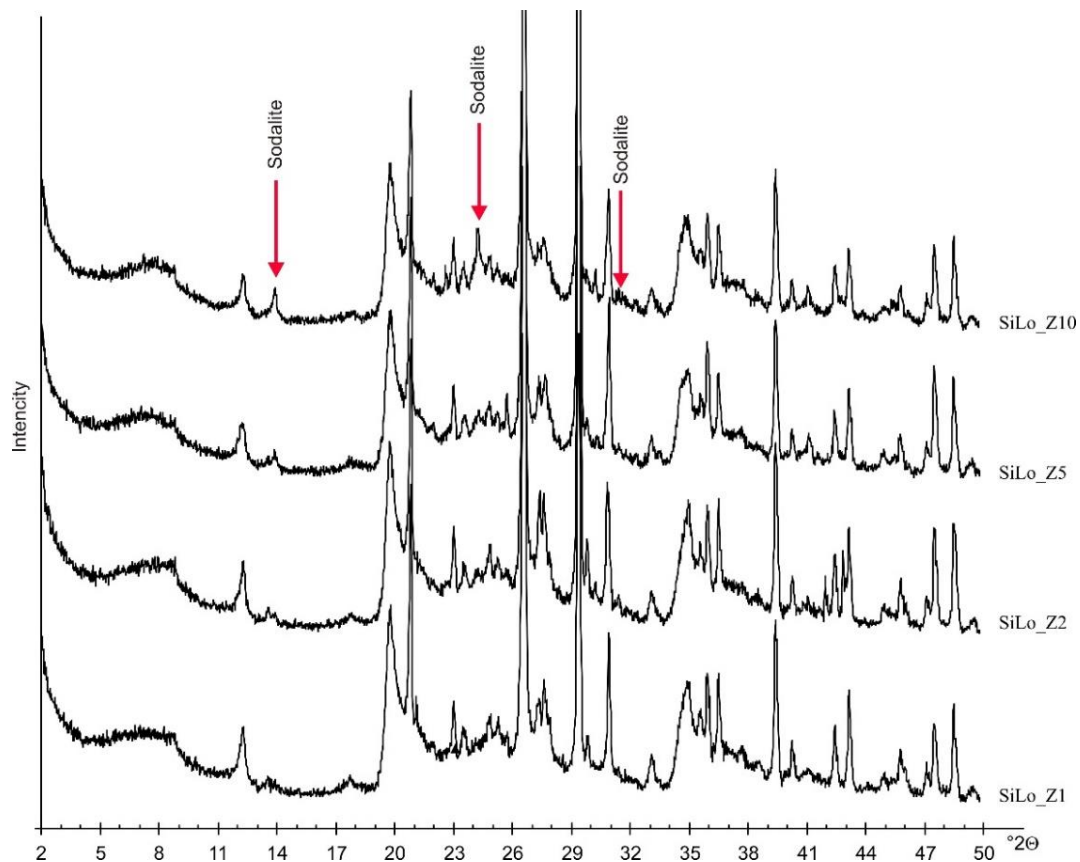**Figure 2.** XRD pattern of zeolite material formed from fly ash.

Figure 3. XRD patterns of soil without zeolite (SiLo_Zo), with 1% (SiLo_Z1), 2% (SiLo_Z2), 5% (SiLo_Z5) and 10% (SiLo_Z10) of zeolite.

The effects determined by the addition of zeolite on the hydrophysical properties of the soil, mainly discussed in the sections below, are due to the typical and specific characteristics of these minerals such as the high pore volumes and low bulk density that modify the soil structure altering bulk density, total porosity, aggregate stability, and average particle size of the final soil mixtures [30].

3.2. Effects of Zeolite on Hydrophysical Properties of Soil

The water retention data collected from the laboratory tests and modeled Equation (1) are illustrated in Figure 4. Data reveal that the presence of zeolite influences the $\theta(h)$ relationship. In general, as the zeolite amount increases in the soil, the experimental SWRCs are shifted upwards with respect to the original (i.e., SiLo_Z0) SWRC. This shift shows that zeolite gives a higher pressure head (h) value for the same soil water content.

It is worth noting that the SWRCs determined for SiLo_Z1 and SiLo_Z2 samples were only slightly influenced by the zeolite treatment. In these two cases, SWRCs only differentiated in the h range between 0 and 0.004 MPa. For h values greater than 0.004 MPa, the curves in practice overlapped with that of SiLo_Z0.

Starting from a soil sample completely saturated with water (which corresponds to a pressure head h equal to zero) the volumetric water content at saturation θ_s grows as the zeolite percentage increases. The θ_s values rise from ~0.610 in the case of the untreated soil sample to ~0.760 for the case of the soil sample mixed with 10% of zeolite. Moving towards higher h values, the amount of water present in the soil is higher in the soil–zeolite mixtures with greater percentages of zeolite. We may infer: "more zeolite, more water". This behavior is not negligible at the lowest zeolite values of 1% and 2%, at least (as mentioned above) in the h range from 0–0.004 MPa, as well as in the other zeolite treatments. From the hydrological point of view, we may conclude that zeolite enhanced the ability of the soil to

retain more water, or in other words, zeolite addition increases the water retention capacity of the soil samples. This is due to high pore volumes and the presence of pore network channels within the zeolite structure and the subsequent ability to hold more water [32].
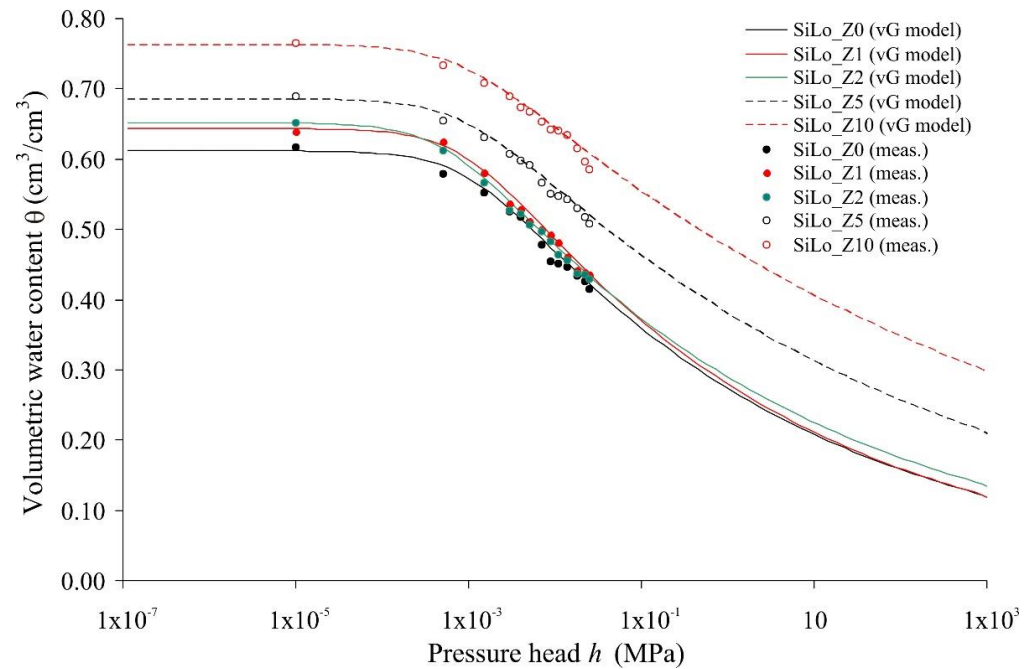

Figure 4. Experimental soil water retention curves (SWRCs) and modeled Equation (1) (van Genuchten, vG model) with reference to the selected soil–zeolite mixtures: SiLo_Z0: soil without zeolite; SiLo_Z1: soil with 1% of zeolite; SiLo_Z2: soil with 2% of zeolite; SiLo_Z5: soil with 5% of zeolite; SiLo_Z10: soil with 10% of zeolite.

Table 2 shows a selection of calculated soil hydrophysical properties, namely: (i) volumetric water content at saturation θ_s, (ii) water content at field capacity θ_{FC} (i.e., the value of θ at $h = -0.03$ MPa), (iii) water content at permanent wilting point θ_{WP} (i.e., the value of θ at $h = -1.5$ MPa), (iv) available water content AWC (i.e., θ_{FC}-θ_{WP}), (v) air capacity AC (i.e., θ_s-θ_{FC}), (vi) hydraulic conductivity at saturation K_s, and (vii) the van Genuchten model parameters α and n. In accordance with Figure 4, the data reported in Table 2 show that θ_{FC} and θ_{WP} increase as the amount of zeolite in the soil increases, with values that vary, respectively, between 0.405 and 0.593, and between 0.255 and 0.456.

Table 2. Soil hydrophysical properties: (i) volumetric water content at saturation (θ_s), (ii) water content at field capacity (θ_{FC}), (iii) water content at permanent wilting point (θ_{WP}), (iv) available water content (AWC), (v) air capacity (AC), (vi) hydraulic conductivity at saturation (K_s), and (vii) van Genuchten's model parameters α and n, obtained from experimental SWRCs and with reference to the selected soil–zeolite mixtures.

Treatments	θ_s (cm³/cm³)	θ_{FC} (cm³/cm³)	θ_{WP} (cm³/cm³)	AWC (cm³/cm³)	AC (cm³/cm³)	K_s (cm/min)	α (1/cm)	n (-)
SiLo_Z0	0.612	0.405 c	0.255 C	0.150	0.207	0.056 A	0.123 a	1.12
SiLo_Z1	0.652	0.417 c	0.272 C	0.145	0.235	0.045 B	0.182 b	1.11
SiLo_Z2	0.644	0.419 c	0.260 C	0.159	0.225	0.028 C	0.155 c	1.12
SiLo_Z5	0.685	0.504 b	0.362 B	0.142	0.181	0.0079 D	0.100 d	1.11
SiLo_Z10	0.763	0.593 a	0.456 A	0.137	0.170	0.0032 E	0.099 d	1.10

Values are means (n = 3). Data were analyzed using one-way ANOVA followed by Duncan Multiple Range Test (DMRT). Within columns means with different uppercase and lowercase letters are significantly different at $p < 0.01$ and at $p < 0.05$, respectively; the lack of letters indicates the lack of significance between means.

For the sake of completeness, we must note that hydraulic conductivity at saturation also changes due to the addition of zeolite. K_s values decreased from 0.056 cm/min (SiLo_Z0) to 0.0032 cm/min (SiLo_Z10); only a small percentage addition of zeolite reduced K_s to 94%. This aspect can be better appreciated with Figure 5, showing the K_{s_TR}/K_{s_UTR} ratios between treated (TR) and untreated (UTR) soil samples.
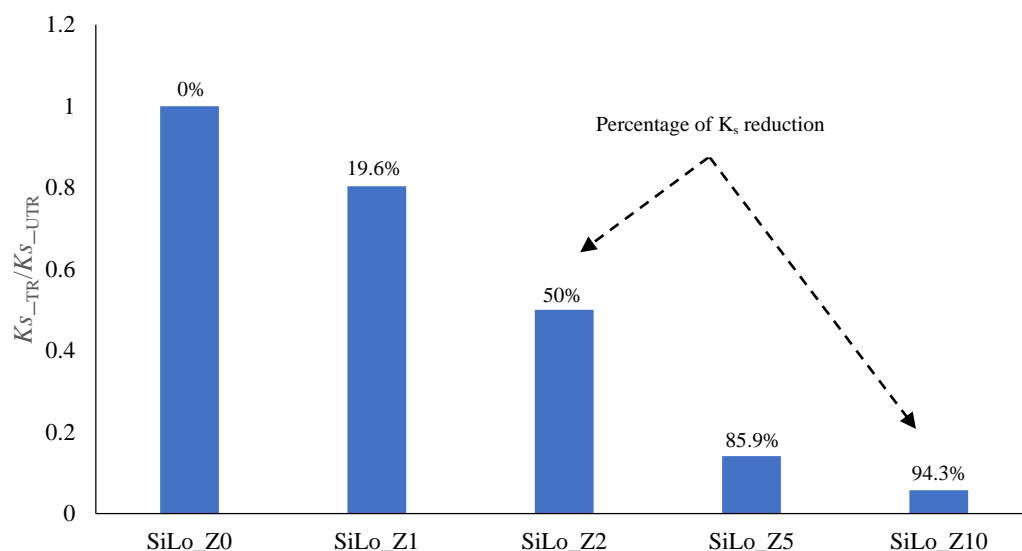

Figure 5. Effects of zeolite on soil hydraulic conductivity at saturation, K_s, determined as the ratio between treated (TR) and untreated (UTR) soil samples. SiLo_Z0: soil without zeolite; SiLo_Z1: soil with 1% of zeolite; SiLo_Z2: soil with 2% of zeolite; SiLo_Z5: soil with 5% of zeolite; SiLo_Z10: soil with 10% of zeolite.

Finally, the graphic in Figure 6 shows the PSDs obtained using Equation (2). The PSD function provides additional information on the mechanisms involved in the soil due to the addition of zeolite. The PSD trend clearly indicates that zeolite modifies the frequency distribution of *h* (or equivalently of the pore sizes). For a fixed *h* value, the *f(h)* function decreases as the zeolite percentage increases; this modification is particularly emphasized in the *h* range from ~0.004 MPa to ~20 MPa.

According to the PSDs and the above-mentioned parameters, as well as the α vG-parameter (that decreases as the zeolite amount increases), we may infer that zeolite favors the formation of a "clay-like" soil due to an increase in meso-micropores combined with macropore loss, thus, limiting the transfer of water and solutes within the soil. These results are consistent with the observed variation in hydrophysical parameters, especially with K_s reduction, and do not conflict with the observed trend of SWRCs. Indeed, increased water retention may be associated not only with large particles and, thus, large pores but also with smaller pores that may contain more water overall but are less conductive [59].

Thus, for the field application of zeolite, these two conflicting effects represented by high water retention capacity and low hydraulic conductivity, should be considered, as also suggested by Yasuda et al. [60].

3.3. Effects of Zeolite on Sunflower Growth

The results of selected sunflower growth parameters on the five different treatments are shown in Figure 7. The data indicate that the treatments with high concentrations of synthetic zeolite (5% and 10%) drastically reduce sunflower growth (SiLo_Z5 and SiLo_Z10) while a concentration of zeolite between 1 and 2% seems to cause a slight decrease in growth (SiLo_Z1 and SiLo_Z2). The variation in plant height of the sunflower is displayed in Figure 7a. The plants that grew in soil treatment without zeolite (SiLo_Z0) and with 1% and 2% of zeolite (SiLo_Z1 and SiLo_Z2) reached their greatest height. Soil treatment with a larger amount of zeolite amendment did not allow the sunflowers to develop

significantly (SiLo_Z5 and SiLo_Z10) since their heights remained quite low. The results also show that, as expected, a higher value of SPAD (59.2) corresponds to the highest zeolite concentration treatment (10%—SiLo_Z10), while no significant variation is observed at lower concentrations (SiLo_Z1 and SiLo_Z2) (Figure 7b). The number of leaves decreased at low concentrations of zeolite (average value is equal to 12), while it more than halved at the zeolite concentration of 10% (SiLo_Z10) (Figure 7c). A similar trend is observed for the leaf area (LA) (Figure 7d). At the end of the experiment, this parameter decreased from 456 cm^2 (value measured without zeolite addition, SiLo_Z0) to 212 cm^2 in SiLo_Z2 and SiLo_Z1, to 67 cm^2 in SiLo_Z5, and to 24 cm^2 in SiLo_Z10. A similar trend also occurred with fresh weight and dry weight values (Figure 7e,f).
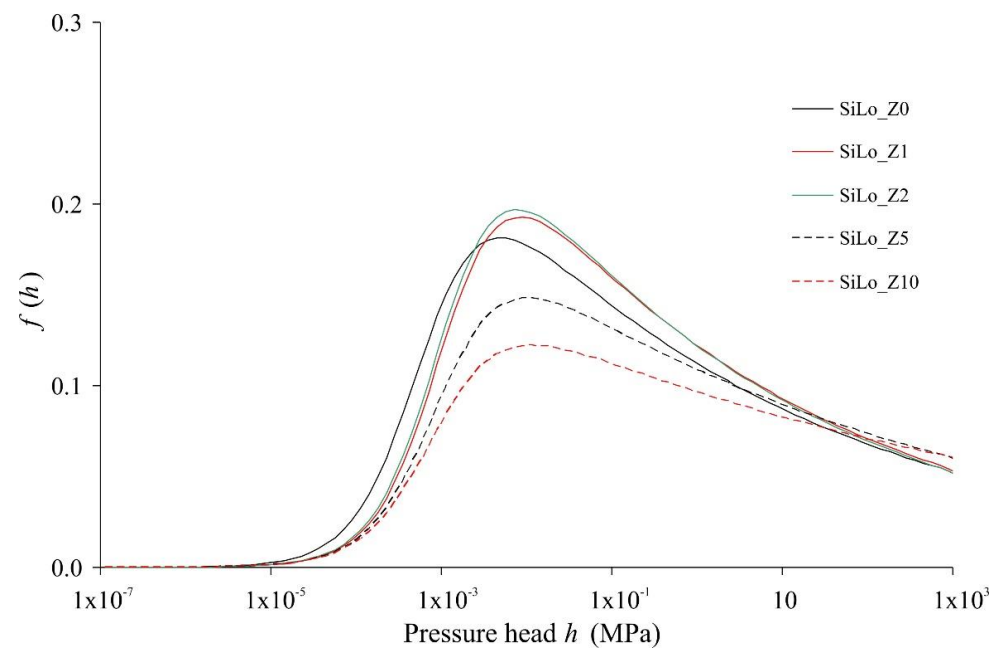

Figure 6. Pore size distribution (PSD) as a function of the pressure head *h* with reference to the selected soil–zeolite mixtures: SiLo_Z0: soil without zeolite; SiLo_Z1: soil with 1% of zeolite; SiLo_Z2: soil with 2% of zeolite; SiLo_Z5: soil with 5% of zeolite; SiLo_Z10: soil with 10% of zeolite.

The increase in soil porosity due to the addition of zeolite generally brings about an improvement in soil structure with potential effects on parameters affecting crop production such as water transport and gas exchange [61]. In contrast to other authors' observations of soils with a sandy texture and on other crops [26,35], we observed a generally negative effect on sunflower growth parameters. There are no data in the literature on crop growth in silty loam soils amended with zeolite, but only positive results on sandy soils [26,35].

The results indicate a positive effect concerning the addition of synthetic zeolite on the soil hydrological constants (θ_{FC} and θ_{WP}) in a silty loam soil. The best conditions for plant growth of sunflower at low concentrations of zeolite (SiLo_Z1 and SiLo_Z2) are supported by the gas exchange parameters of these treatments which showed values of stomatal conductance close to the untreated control (0.37 mol H$_2$O m^{-2} s^{-1} on average for SiLo_Z0, SiLo_Z1, and SiLo_Z2 vs. 0.18 mol H$_2$O m^{-2} s^{-1} on average for SiLo_Z5 and SiLo_Z10; data not shown). Sunflower growth response confirms what was observed on the SWRC curve modification, especially for treatments amended with 5% and 10% of zeolite (Figure 4). Modification of the SWRCs determines a variation in the soil's moisture range at which water is available for plants (Table 2). At the wilting point, the soil pressure is usually −1.5 MPa; this is the value where soil's water is bound to the soil and not available for plants. As discussed above, treatment with zeolite brings about a modification of the soil's porosity and aggregates, with an overall increase in mesopores and micropores combined with macropore loss. As a consequence, water, especially in the micropores, is

less available for plants because the pressure becomes more negative as the pore radius decreases (Figures 4 and 6).
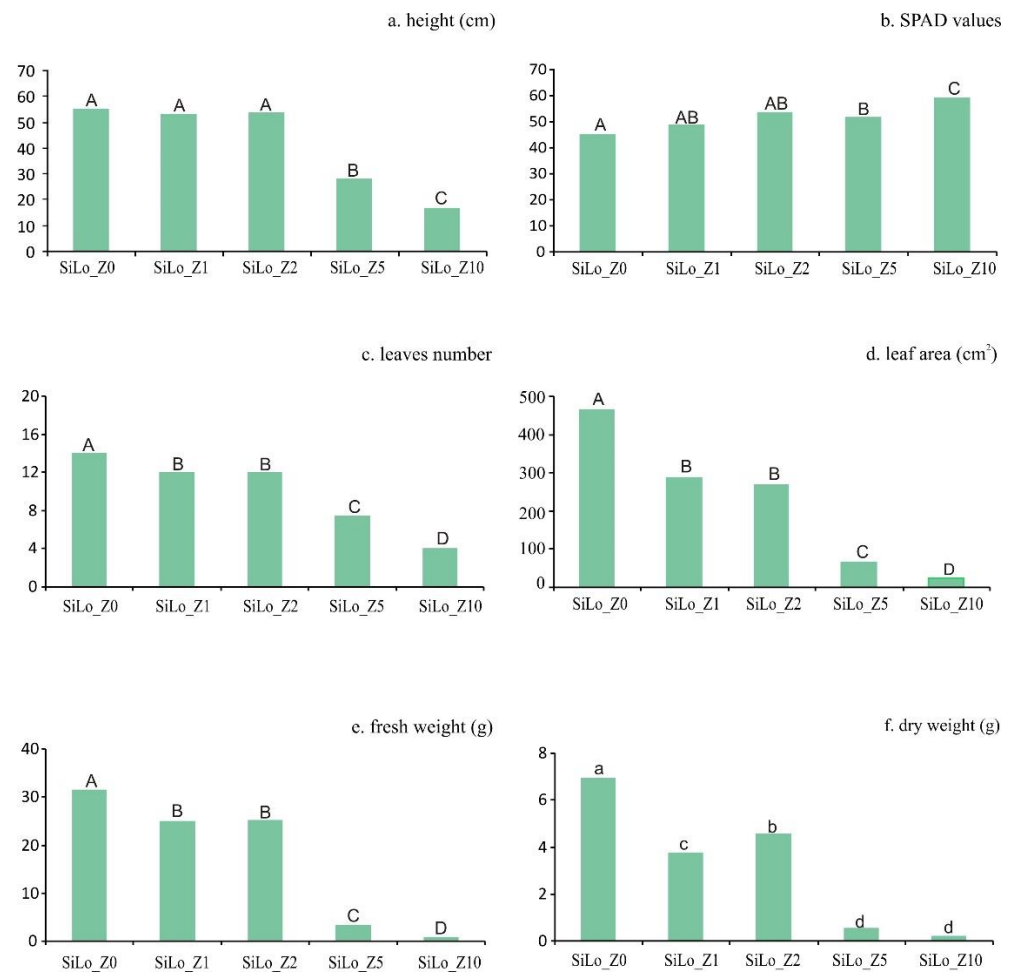

Figure 7. (**a**) Plant height, (**b**) SPAD values, (**c**) leaf number, (**d**) leaf area, (**e**) fresh weight, and (**f**) dry weight of sunflower plant at the flower bud stage, grown on soil treated with different percentages of zeolite (0–10%). Values are means (n = 6). Data presented in each graph were analyzed by one-way ANOVA followed by DMRT. Different uppercase and lowercase letters above the bars are significantly different at $p < 0.01$ and at $p < 0.05$, respectively. SiLo_Z0: soil without zeolite; SiLo_Z1: soil with 1% of zeolite; SiLo_Z2: soil with 2% of zeolite; SiLo_Z5: soil with 5% of zeolite; SiLo_Z10: soil with 10% of zeolite.

As a result of the variation in the pore size distribution, the wilting point passes from 26% to 46% and the field capacity from 41% to 59% in the SiLo_Z0 and in the SiLo_Z10, respectively (Table 2). The lower K_s of soil with 5% and 10% of zeolite negatively affects the growth parameters characterizing SiLo_Z5 and SiLo_Z10 such as leaf number, leaf area, fresh weight, and dry weight which stand at significantly lower values (Figure 7a–f). However, leaf number, leaf area, fresh weight, and dry weight of the sunflower plants also resulted in being significantly lower with 1 and 2% of zeolite than untreated soil (Figure 7c–f). Interestingly, as also hypothesized in the literature [9], the highest percentage of zeolite in the soil causes a "self-saturation" effect of the zeolite, which ends up retaining water within itself rather than releasing it and making it available to plants. Due to the addition of zeolite, we observed a great increase in the soil water content in correspondence with the wilting point in the treatment containing 10% of zeolite (SiLo_Z10, see Table 2). In SiLo_Z2, we also observed the minor shift in soil moisture values in correspondence with the hydrological constants of untreated soil (i.e., the wilting point and field capacity).

According to other authors [13,26,35], SWRC modification due to zeolite addition brings about a change in AWC, particularly in sandy soil. The impact of zeolite on pore radius and hydrophysical parameters, especially K_s reduction, can result in plant water unavailability, a condition which negatively impacts crop growth. Other authors have also shown that the effectiveness of water-retention amendments for improving plant available water varies in different soils or substrates [62]. In other words, the effect of zeolite on cultivated soils strongly depends on the amount added but, overall, on the texture of the soil. The negative outcome of adding zeolite to a silty loam soil on crop growth closely depends on the reduction of drainage capacity and on the shift of the water availability range towards higher soil humidity values, especially if zeolite is added in large amounts.

4. Conclusions

In the present research, we investigated the effects of a zeolite, synthesized from an Italian coal fly ash sample (a waste material), on the hydrophysical properties of soil, a typical silty loam soil of Southern Italy, and on sunflower growth, which was selected as a reference plant. To analyze these aspects, several experiments were carried out at laboratory-scale, on selected soil–zeolite mixtures of 1%, 2%, 5%, and 10%, following the experimental protocols described in Section 2.

The results indicated that zeolite addition increases the water retention capacity of soil, and, on the other hand, decreases the drainage capacity (K_s reduces as zeolite increases). These effects may be mainly attributed to the deviation of the initial pore size distribution (PSD) of the amended soils that reassembled their internal structure, promoting the formation of a "clay-like" soil. The conclusion is that PSD modification causes a variation in the range of available water towards higher values of soil humidity as the amount of added zeolite increases.

The research in question requires additional experiments and datasets, even at full field-scale, to extend the observed results in different pedological contexts of agronomic interest. However, it also yields preliminary insights in terms of policies linked to the circular economy: the possibility of synthesizing zeolites from fly ash for agricultural purposes could bring about a substantial reduction in the amounts of this waste product taken to landfill.

Author Contributions: Conceptualization, Formal analysis, Writing—original draft, C.B.; Conceptualization, Formal analysis, Writing original draft, A.S.; Conceptualization, Formal analysis, Writing original draft, S.L.; Conceptualization, Formal analysis, Writing original draft A.C. (Alessandro Comegna); Writing original draft, A.C. (Antonio Coppola); Formal analysis, G.D.; Writing—original draft, F.C.; Conceptualization, Formal analysis, Writing—original draft, A.R.R. All authors have read and agreed to the published version of the manuscript.

References

1. Huang, Z.B.; Zhanbin, H. Zeolite application for enhancing water infiltration and retention in loess soil. *Resour. Conserv. Recycl.* **2001**, *34*, 45–52.
2. Wang, Y.; Li, S.; Quin, S.; Hui, G.; Young, D.; Lam, H.M. How can drip irrigation save water and reduce evapotranspiration compared to border irrigation in arid regions in northwest China. *Agr. Water Manag.* **2001**, *239*, 1062560. [CrossRef]
3. Paknejad, F.; Nasri, M.; Moghadam, H.R.T.; Zahedi, H.; Alahmadi, M.J. Effects of drought stress on chlorophyll fluorescence parameters, chlorophyll content and grain yield of wheat cultivars. *J. Biol. Sci* **2007**, *7*, 841–847. [CrossRef]
4. Juri, W.A.; Vaux, H., Jr. The role of sciencein solving the world's emerging water problems. *Proc. Natl. Acad. Sci. USA* **2005**, *102*, 15715–15720. [CrossRef]
5. Krumm, M.; Guillaume, J.H.A.; De Moel, H.; Eisner, S.; Flörke, M.; Porkka, M.; Siebert, S.; Veldkamp, T.I.E.; Ward, P.J. The world's road to water scarcity: Shortage and stress in the 20th century and pathways towards sustainability. *Sci. Rep.* **2016**, *6*, 38495.
6. Gerveni, M.; Avelino, A.F.T.; Dall'erba, S. Drivers of Water Use in the Agricultural Sector of the European Union 27. *Environ. Sci. Technol.* **2020**, *54*, 9191–9199. [CrossRef]

7. Khan, M.A.A.; Mahmood, K.; Ashraf, I.; Siddiqui, M.T.; Knox, J.W. Evaluating socio-economic and environmental factors influencing farm-level water scarcity in Punjab, Pakistan. *Irrig. Drain* **2020**, *70*, 797–808. [CrossRef]
8. Demitri, C.; Scalera, F.; Madaghiele, M.; Sannino, A.; Maffezzoli, A. Potential of cellulose-based superabsorbent hydrogels as water reservoir in agriculture. *Int. J. Polym. Sci.* **2013**, *12*, 435073. [CrossRef]
9. Cannazza, G.; Cataldo, A.; De Benedetto, E.; Demitri, C.; Madaghiele, M.; Sannino, A. Experimental assessment of the use of a novel superabsorbent polymer (SAP) for the optimization of water consumption in agricultural irrigation process. *Water* **2014**, *6*, 2056–2069. [CrossRef]
10. Satriani, A.; Catalano, M.; Scalcione, E. The role of superabsorbent hydrogel in bean crop cultivation under deficit irrigation conditions: A case-study in Southern Italy. *Agric. Water Manag.* **2018**, *195*, 114–119. [CrossRef]
11. Ai, F.; Yin, X.; Hu, R.; Ma, H.; Liu, W. Research into the super-absorbent polymers on agricultural water. *Agric. Water Manag.* **2021**, *245*, 106513. [CrossRef]
12. Alghamdi, A.G.; Alkhasha, A.; Ibrahim, H.M. Effect of biochar particle size on water retention and availability in a sandy loam soil. *J. Saudi Chem. Soc.* **2020**, *24*, 1042–1050. [CrossRef]
13. de Campos Bernardi, A.C.; Peronti Anchao Oliviera, P.; de Melo Monte, M.B.; Souza-Barros, F. Brazilian sedimentary zeolite use in agriculture. *Micropor. Mesopor. Mat.* **2013**, *167*, 16–21. [CrossRef]
14. Mondal, M.; Biswas, B.; Garai, S.; Sarkar, S.; Banerjee, H.; Brahmachari, K.; Bandyopadhyay, P.K.; Maitra, S.; Brestic, M.; Skalicky, M.; et al. Zeolites enhance soil health, crop productivity and environmental safety. *Agronomy* **2021**, *11*, 448. [CrossRef]
15. Belviso, C.; Cavalcante, F.; Ragone, P.; Fiore, S. Immobilization of Ni by synthesising zeolite at low temperatures in a polluted soil. *Chemosphere* **2010**, *78*, 1172–1176. [CrossRef]
16. Belviso, C.; Cavalcante, F.; Ragone, P.; Fiore, S. Immobilization of Zn and Pb in polluted soil by in-situ crystallization zeolites from fly ash. *Water Air Soil Pollut.* **2012**, *223*, 5357–5364. [CrossRef]
17. Matthew, D.O.; Soltis, J.A.; Marlon, T.C.; Lee Penn, R.; Rimer, J.D. Nucleation of FAU and LTA zeolites from heterogeneous aluminosilicate precursors. *Chem. Mater.* **2016**, *28*, 4906–4916.
18. Belviso, C. EMT-type zeolite synthesized from obsidian. *Micropor. Mesopor. Mat.* **2016**, *226*, 325–330. [CrossRef]
19. Belviso, C. Ultrasonic vs hydrothermal method: Different approaches to convert fly ash into zeolite. How they affect the stability of synthetic products over time? *Ultrason. Sonochem.* **2018**, *43*, 9–14. [CrossRef]
20. Ng, E.-P.; Awala, H.; Tan, K.-H.; Adam, F.; Retoux, R.; Mintova, S. EMT-type zeolite nanocrystals synthesized from rice husk. *Micropor. Mesopor. Mat.* **2015**, *204*, 2014–2209. [CrossRef]
21. Belviso, S.; Cavalcante, F.; Lettino, A.; Ragone, P.; Belviso, C. Fly ash as raw material for the synthesis of zeolite-encapsulated porphyrazine and metallo porphyrazine tetrapyrrolic macrocycles. *Micropor. Mesopor. Mat.* **2016**, *236*, 228–234. [CrossRef]
22. Shahsavari, N. Effects of Zeolite and Zinc on Quality of Canola (*Brassica napus* L.) Under Late Season Drought Stress. Commun. *Soil Sci. Plant Anal.* **2019**, *50*, 1117–1122. [CrossRef]
23. Belviso, C.; Cavalcante, F.; Niceforo, G.; Lettino, A. Sodalite, faujasite and A-type zeolite from 2:1dioctahedral and 2:1:1 trioctahedral clay minerals. A singular review of synthesis methods through laboratory trials at a low incubation temperature. *Powder Technol.* **2017**, *320*, 483–497. [CrossRef]
24. Sepaskhah, A.R.; Barzegar, M. Yield, water and nitrogen-use response of rice to zeolite and nitrogen fertilization in a semi-arid environment. *Agric. Water Manag.* **2010**, *98*, 38–44. [CrossRef]
25. Najafinezhad, H.; Tahmasebi-Sarvestani, Z.; Modarres Sanavy, S.A.M.; Naghavi, H. Evaluation of yield and some physiological changes in corn and sorghum under irrigation regimes and application of barley residue, zeolite and superabsorbent polymer. *Arch. Agron. Soil Sci.* **2014**, *61*, 891–906. [CrossRef]
26. Ippolito, A.J.; Tarkalson, D.D.; Lehrsch, G.A. Zeolite soil application method affects inorganic nitrogen, moisture, and corn growth. *Soil Sci.* **2011**, *176*, 136–142. [CrossRef]
27. Al-Busaidi, A.; Yamamoto, T.; Tanigawa, T.; Rahman, H.A. Use of zeolite to alleviate water stress on subsurface drip irrigated barley under hot environments. *Irrig. Drain.* **2011**, *60*, 473–480. [CrossRef]
28. Hazrati, S.; Tahmasebi-Sarvestani, Z.; Mokhtassi-Bidgoli, A.; Modarres-Sanavya, S.A.M.; Mohammadi, H.; Nicola, S. Effects of zeolite and water stress on growth, yield and chemical compositions of *Aloe vera* L. *Agric. Water Manag.* **2017**, *181*, 66–72. [CrossRef]
29. Gholizadeh, A.; Amin, M.S.M.; Anuar, A.R.; Saberioon, M.M. Water stress and natural zeolite impacts on phisiomorphological characteristics of moldavian balm (*Dracocephalum moldavica* L.). *Aust. J. Basic Appl. Sci.* **2010**, *4*, 5184–5190.
30. Nakhli, S.A.A.; Delkash, M.; Bakhshayesh, B.E.; Kazemian, H. Application of zeolites for sustainable agriculture: A review on water and nutrient retention. *Water Air Soil Pollut* **2017**, *228*, 464–497. [CrossRef]
31. Szerement, J.; Ambrożewicz-Nita, A.; Kędziora, K.; Piasek, J. Use of zeolite in agriculture and environmental protection. A short review. *Вісник Національного Університету* **2014**, *781*, 172–177.
32. Ramesh, K.; Reddy, D.D. Chapter four—Zeolites and their potential uses in agriculture. *Adv. Agron.* **2011**, *113*, 219–241.
33. Chmielewska, E. Designing clinoptiloliterich tuff columns for adsorptive filtration of water with enhanced ammonium concentration. *Fresenius Environ. Bull.* **2014**, *24*, 1277–1283.
34. Bernardi, A.D.C.; Mendonça, F.; Haim, P.; Werneck, C.; Monte, M.D.M. Water availability and rice yield due to levels of zeolitic concentrate. *Irriga* **2009**, *14*, 123–134. [CrossRef]

35. Demir, A.; Gunay, A.; Debik, E. Ammonium removal from aqueous solution by ion exchange using packed bed natural zeolite. *Water SA* **2002**, *28*, 329–336. [CrossRef]
36. Piñón-Villarreal, A.R.; Bawazir, A.S.; Shukla, M.K.; Hanson, A.T. Retention and transport of nitrate and ammonium in loamy sand amended with clinoptilolite zeolite. *J. Irrig. Drain. Eng.* **2013**, *139*, 755–765. [CrossRef]
37. Zwingmann, N.; Singh, B.; Mackinnon, I.D.; Gilkes, R.J. Zeolite from alkali modified kaolin increases NH 4 retention by sandy soil: Column experiments. *Appl. Clay Sci.* **2009**, *46*, 7–12. [CrossRef]
38. Zheng, J.; Chen, T.; Wu, Q.; Yu, J.; Chen, W.; Che, Y.; Siddique, K.H.M.; Meng, W.; Chi, D.; Xia, G. Effect of zeolite application on phenology, grain yield and grain quality in rice under water stress. *Agric. Water Manag.* **2018**, *206*, 241–251. [CrossRef]
39. Polat, E.; Karaca, M.; Demir, H.; Naci Onus, A. Use of natural zeolite (clinoptilolite) in agriculture. *J. Fruit Ornam. Plant Res.* **2004**, *12*, 183–189.
40. Ozbahce, A.; Tari, A.F.; Gonulal, E.; Simsekli, N. Zeolite for Enhancing Yield and Quality of Potatoes Cultivated Under Water-Deficit Conditions. *Potato Res.* **2018**, *61*, 247–259.
41. Bahador, M.; Tadayon, M.R. Investigating of zeolite role in modifying the effect of drought stress in hemp: Antioxidant enzymes and oil content. *Ind. Crop. Prod.* **2020**, *144*, 112042. [CrossRef]
42. Belviso, C. State-of-the-art applications of fly ash from coal and biomass: A focus on zeolite synthesis processes and issues. *Progr. Energy Combust. Sci.* **2018**, *65*, 109–135. [CrossRef]
43. Ayan, S.; Yahyaoglu, Z.; Gercek, V.; Sahin, A. Utilization of zeolite as a substrate for containerised oriental spruce (*Picea orientalis* L.) seedlings propagation. *Int. Symp. Grow. Media* **2008**, *779*, 583–890.
44. Flores, C.G.; Schneider, H.; Marcilio, N.R.; Ferret, L.; Oliveira, J.C.P. Potassic zeolites from Brazilian coal ash for use as a fertilizer in agriculture. *Waste Manag.* **2017**, *70*, 263–271. [CrossRef]
45. Kottek, M.; Grieser, J.; Beck, C.; Rudolf, B.; Rubel, F. World map of the Köppen-Geiger climate classification updated. *Meteorol. Z.* **2006**, *15*, 259–263. [CrossRef]
46. Official Gazette of the Italian Republic, General Series n° 248, 1999, Ordinary Supplement n° 12. Available online: www.ecochimicasas.it/web/data/uploads/files/d.m.-13_set_99-metodi-di-analisi-chimica-del-suolo.pdf (accessed on 10 January 2022).
47. *ASTM D422-63*; Standard Test Method for Particle-Size Analysis of Soils. ASTM International: West Conshohocken, PA, USA, 2007.
48. Belviso, C.; Cavalcante, F.; Fiore, S. Synthesis of zeolite from Italian coal fly ash. Differences in crystallization temperature using seawater instead of distilled water. *Waste Manag.* **2010**, *30*, 839–847. [CrossRef]
49. Sun, H.; Wu, D.; Guo, X.; Navrotsky, A. Energetic and structural evolution of Na-Ca exchanged zeolite A during heating. *Phys. Chem. Chem. Phys* **2015**, *17*, 9241–9247. [CrossRef]
50. Klute, A.; Dirksen, C. Hydraulic conductivity and diffusivity. Laboratory methods. In *Methods of Soil Analysis—Part 1. Physical and Mineralogical Methods*, 2nd ed.; Klute, A., Ed.; SSSA: Madison, WI, USA, 1986; pp. 687–734. [CrossRef]
51. Stackman, W.P.; Valk, G.A.; van der Harst, G.G. *Determination of Soil Moisture Retention Curves: I. Sand Box Apparatus*; Range, P.F., Ed.; ICW: Wageningen, The Netherlands, 1969; p. 119.
52. van Genuchten, M.T.H. A closed-form equation for predicting the hydraulic conductivity of unsaturated soils. *Soil Sci. Soc. Am. J.* **1980**, *44*, 892–898. [CrossRef]
53. van Genuchten, M.T.H.; Leij, F.T.; Yates, S.R. *The RETC Code for Quantifying the Hydraulic Functions of Unsaturated Soils*; Rep. EPA/600/2-91/065; U.S. Environmental Protection Agency: Ada, OK, USA, 1991.
54. Comegna, A.; Dragonetti, G.; Kodesova, R.; Coppola, A. Impact of olive mill wastewater (OMW) on the soil hydraulic and solute transport properties. *Int. J. Environ. Sci. Technol.* **2021**. [CrossRef]
55. Durner, W. Hydraulic conductivity estimation for soils with heterogeneous pore structure. *Water Resour. Res.* **1994**, *30*, 211–223. [CrossRef]
56. Jensen, K.L.; Watts, C.W.; Christensen, B.T.; Munkholm, L.J. Soil Water Retention: Uni-Modal Models of Pore-Size Distribution Neglect Impacts of Soil Management. *Soil Sci. Soc. Am. J.* **2019**, *83*, 18–26. [CrossRef]
57. Kosugi, K. Three-parameter lognormal distribution model for soil water retention. *Water Resour. Res.* **1994**, *30*, 891–901. [CrossRef]
58. Nimmo, J.R. Porosity and Pore Size Distribution. In *Encyclopedia of Soils in the Environment*; Hillel, D., Ed.; Elsevier: London, UK, 2004; pp. 295–303.
59. Nimmo, J.R. Porosity and Pore Size Distribution. In *Reference Module in Earth Systems and Environmental Sciences*; Elsevier: Amsterdam, The Netherlands, 2013. [CrossRef]
60. Yasuda, H.; Takuma, K.; Fukuda, T. Water retention changes of dune sand due to zeolite addition. *J. Agric. Meteorol.* **1997**, *52*, 641–644. [CrossRef]
61. Skopp, J.; Gardner, W.R.; Tyler, E.J. Solute movement in structure soils: Two region model with small interaction. *Soil Sci. Soc. Am. J.* **1981**, *5*, 461–472.
62. Akhter, J.; Mahmood, K.; Malik, K.A.; Mardan, A.; Ahmad, M.; Iqbal, M.M. Effects of hydrogel amendment on water storage of sandy loam and loam soils and seedling growth of barley, wheat and chickpea. *Plant Soil Environ.* **2004**, *50*, 463–469. [CrossRef]